International Journal of Recent Technology and Engineering (IJRTE)
ISSN: 2277-3878 (Online), Volume-9 Issue-2, July 2020

Efficient Machine Learning Techniques to Detect Glaucoma using Structure and Texture based Features

Nataraj Vijapur, R. Srinivasa Rao Kunte

Abstract: ***Survey of world health organization has revealed that retinal eye disease Glaucoma is the second leading cause for the blindness worldwide. It is the disease which will steal the vision of the patient without any warning or symptoms. About half of the world Glaucoma patients are estimated to be in Asia. Hence, for social and economic reasons, Glaucoma detection is necessary in preventing blindness and reducing the cost of surgical treatment of the disease. The objective of the paper is to predict and detect Glaucoma efficiently using image processing and machine learning based classification techniques. Segmentation techniques such as unique template approach, Gray Level Coherence Matrix based feature extraction approach and wavelet transform based approach are used to extract these structure and texture based features. Combination of structure based and texture based techniques along with machine learning techniques improves the efficiency of the system. Developed efficient Computer aided Glaucoma detection system classifies a fundus image as either Normal or Glaucomatous image based on the structural features of the fundus image such as Cup-to-Disc Ratio (CDR), Rim-to-Disc Ratio (RDR), Superior and Inferior neuro-retinal rim thicknesses, Vessel structure based features and Distribution of texture features in the fundus images.***

Keywords: GLCM, Glaucoma, Cup-to-Disc Ratio (CDR), Rim-to-Disc Ratio (RDR), Image Processing, Machine Learning, Structure features and Texture features.

I. INTRODUCTION

According to the survey of World Health Organization, over the last ten years cataract remains the highest leading cause of blindness worldwide covering 47.9% of overall blindness. It is a progressive and painless clouding of the internal lens of the eye. Similarly, the survey declares Glaucoma as the second leading cause for the blindness worldwide. About 12.3% of patients in the world are suffering from Glaucoma [1].

Manuscript received on May 25, 2020.
Revised Manuscript received on June 29, 2020.
Manuscript published on July 30, 2020.
***** Correspondence Author
Nataraj Vijapur*, Electronics & Communication Department, KLE Dr.M.S.Sheshgiri College of Engg & Technology, Belagavi, Karnataka, India. E-mail: nvijapur@gmail.com
Srinivasa Rao Kunte, Electronics & Communication Department, Sahyadri College of Engineering & Management, Mangalore, India. E-mail: kuntesrk@gmail.com

It is a disease which will steal the vision of the patient without any warning or symptoms. Surveys conducted in North America and Europe revealed a significant proportion of new Glaucoma patients who were previously gone undetected. Proportion estimated for Glaucoma patients in Asia and developing countries is even larger [2]. This calls for the need for early Glaucoma detection and we can prevent blindness and reduce the surgical cost involved in treating the disease. The fundus . image of the eye, Glaucoma disease, structural changes in fundus image due to Glaucoma and its diagnosis are presented in this section.

A. Fundus Image

Eye is the most complex organ of the human body with approximate dimension of 2.54 cm width, 2.3 cm height and 2.54 cm deep [3]. Human eye acts like a camera [4] and processes the visual signals. Figure 1 shows the front view of eye fundus image consisting of Optic Disc and Optic Cup. The optic nerves and blood vessels exit the retina from optic disc. It is considered as one of the main features of a retinal fundus image and is located to the nasal side of the fovea. It is vertically oval, with an average dimension of horizontally 1.76 mm and vertically 1.92 mm. In-side the optic disc there is a central depression, of variable size, called the Optic Cup.

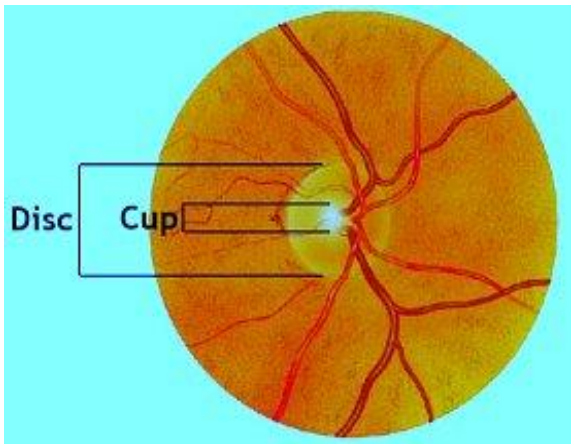

Fig. 1. Front view of eye fundus image

The optic nerve head is the location where ganglion cell axons exit the eye to form the optic nerve. The change in the shape and color or depth of optic disc and optic cup are the indicators of various ophthalmic pathologies especially for Glaucoma and other eye diseases. Optic disc and cup are the brightest features of the normal fundus. The disc appears to be as a bright yellow or white region in colored fundus image.

B. Structural changes in Fundus Image due to Glaucoma

The structure and appearance of the optic disc can reveal the presence of Glaucoma and they are considered as very important features to assess the damage due to Glaucoma. The optic cup concentric enlargement, decrease in rim area and other such patterns of Glaucomatous damage are most commonly found.

The ratio of area of optic cup to area of optic disc is normally considered to evaluate the disease. Due to Glaucoma, in the retina the optic cup area enlarges and progresses towards the disc. This distinction can be seen between normal and Glaucoma affected fundus images as shown in Figure 2(a) and 2(b), respectively. This Cup-to-Disc area Ratio (CDR) is used in ophthalmology to determine the progression of Glaucoma. If the CDR value is greater than 0.3, the patient has a threat of Glaucoma. The CDR of the image in Figure 2(b) is nearly 0.7 and it is a prominent case of Glaucoma.

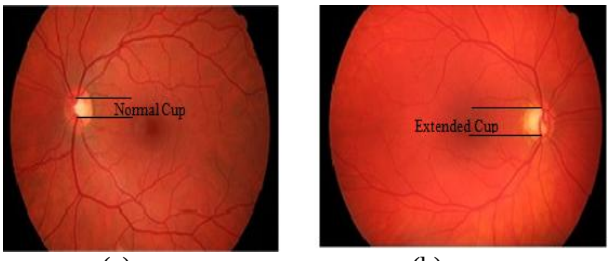

(a) (b)

Fig. 2. Fundus images (a) normal eye (b) Glaucoma eye

The area present between the cup and disc boundary of the eye is termed as Neuro-retinal rim [5] as shown in Figure 3(a) and (b) for a sample of normal and Glaucoma eye, respectively. Thinning of the neuroretinal rim is also one of the symptoms of the Glaucoma. Rim-to-Disc area Ratio (RDR) is also an indicator for Glaucoma. As seen from Figure 3, normal eye has more RDR compared to Glaucoma eye.

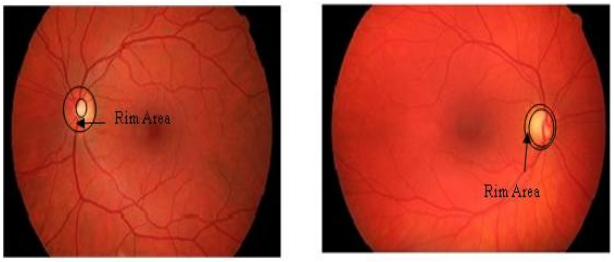

(a) (b)

Fig. 3. Neuroretinal rim (a) rim area in normal eye (b) rim area in Glaucoma eye

The retinal image shall be seen as composed of Inferior, Superior, Nasal and Temporal regions as shown in Figure 4(a). Due to Glaucoma, blood vessels covered by the nasal region increases and Inferior-Superior region decreases. Hence, the ratio of the area of sum of blood vessels in the Inferior-Superior region to the sum of blood vessels in the Nasal-Temporal region (ISNT) decreases. This feature can also be used to detect Glaucoma more accurately [5], [6].

A study has revealed that the diameters of the retinal vessels been seen to be significantly smaller in Glaucomatous eyes compared to normal eyes [7], [8]. This reduction in vessel diameters can be continuously monitored and disease can be detected in early stages. Also, in case of prominent cases of Glaucoma there is a distortion observed in cup structure. Cup usually expands downwards more towards inferior side. Therefore, disease can be detected by measuring the difference in neuroretinal rim thickness at Superior and Inferior regions, which are referred as Superior rim thickness and Inferior rim thickness as shown in Figure 4(b).

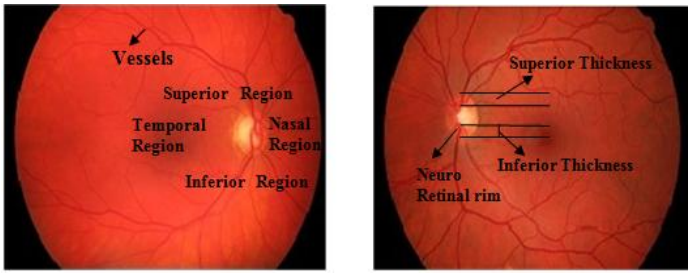

(a) (b)

Fig. 4. Regions of fundus image (a) ISNT regions and vessels (b) neuroretinal rim and Superior and Inferior thicknesses

In case of Glaucoma thickness of the vessels around the disc goes on reducing due to lack of fresh Aqueous humor. This also results in disappearance of small vessels around the disc. Normal eye contains a lot of very minute vessels like small branches of tree around the optic disc, which are absent in Glaucoma eye as shown in Figure 5.

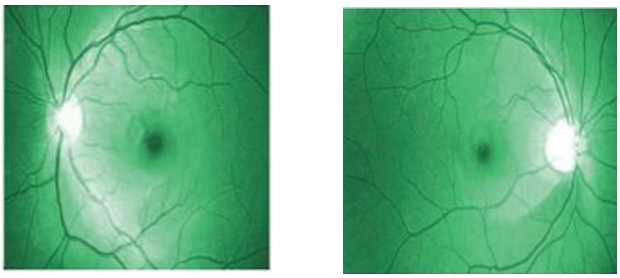

(a) (b)

Fig. 5. Vessels in fundus image (a) normal eye as seen through the green filter (b) Glaucoma eye in green filter

In normal eye peripheral vision is present fully. In Glaucoma affected eye peripheral vision goes on reducing. As an illustration, Figure 6(a) shows the vision of a sample picture as perceived by a normal eye and Figure 6(b) shows the vision of the same picture as perceived by a Glaucoma eye.

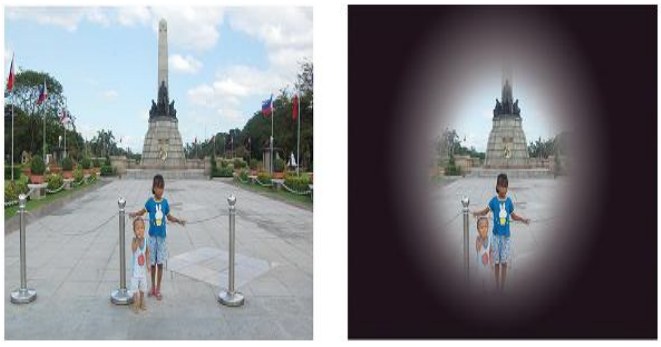

(a) (b)

Fig. 6. Vision loss due to Glaucoma (a) normal eye vision (b) Glaucoma eye vision
(Courtesy: http://www.caeps.org/)

C. Fundus Features used for Glaucoma Detection

We propose to use the fundus features such as (i) CDR (ii) RDR (iii) Superior rim thickness (iv) Inferior rim thickness and (v) Structural features of vessels around the disc such as maximum vessel diameter, number of vessel segments and total number of smaller diameters of vessels (vi) spatial textures to detect Glaucoma by the digital image processing techniques.

II. PROPOSED COMPREHENSIVE EFFICIENT INTEGRATED GLAUCOMA DETECTION SYSTEM

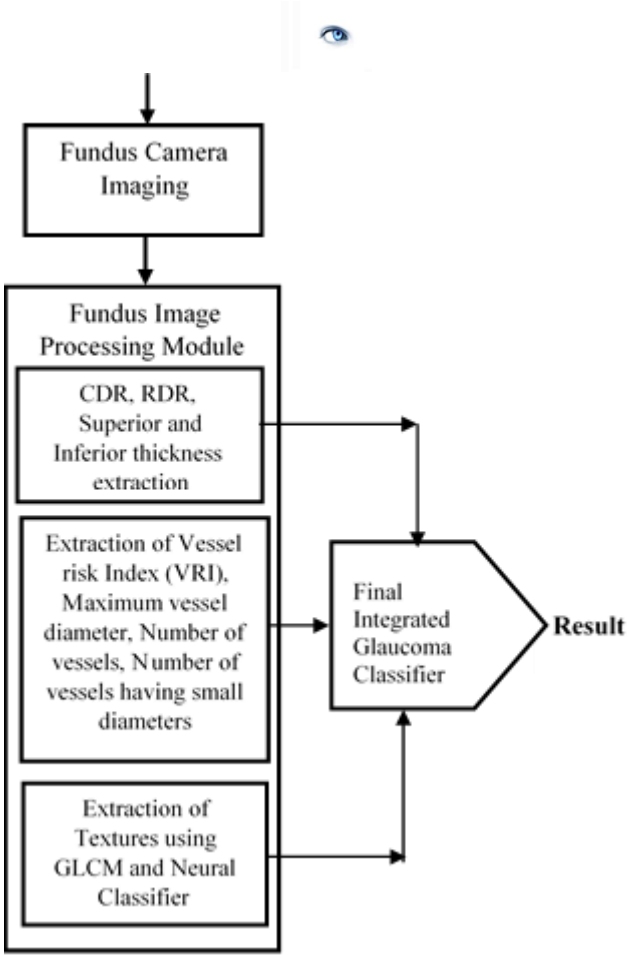

Fig. 7 Schematic of the Final Integrated System

The block schematic of our proposed comprehensive efficient integrated Glaucoma detection system for Glaucoma identification using image processing techniques is shown in Figure 7. The retinal image of the eye is captured using a fundus camera. The captured eye fundus image is subjected to various image processing techniques to extract different features of fundus image. Our proposed system extracts and uses the following three different sets of fundus eye image features for detection of Glaucoma. Fundus structure based features such as CDR, RDR and Neuroretinal rim thicknesses Vessel structural features and Textural features.

Structure based features of fundus image are extracted using a template based approach. A template aids the segmentation of optic cup and disc from the fundus image. Template is correlated with fundus image using Pearson-r correlation for segmentation. Structure based features such as CDR, RDR, Superior and Inferior rim thicknesses are extracted.

Fundus images' vessel structure based features such as vessel count, vessel diameters, maximum vessel diameter, and count of vessels having fewer diameters are extracted using Isotropic Un-decimated Wavelet Transform (IUWT) [8],[28].

Grey Level Co-occurrence Matrix based texture features of Fundus images' are extracted. Features Contrast, Correlation, Energy, Homogeneity and Entropy are extracted. A trained neural classifier fed with the texture features classifies the given test image into a Normal or Glaucoma image as the first stage of classification.

Based on the literature survey and suggestion of ophthalmologists, the ultimate Glaucoma classifier is developed. The above set of extracted features and neural classifier output are fed to the final classifier. It finally classifies the given test image as either (i) Normal or (ii) Glaucoma or (iii) Acute Glaucoma or (iii) Early Glaucoma Symptoms image.

The extracted features like CDR, RDR, Superior rim thickness and Inferior rim thicknesses, Vessel count, Vessel diameter, Maximum vessel diameter, Count of vessels having fewer diameters are stored in a database meant for the patient. These features can be used to assess the progression of the disease during the next visit of the patient. This will assist the ophthalmologists for better monitoring of patients. Database will be very useful for mass screening programs and also plays an important role in detecting Glaucoma at an early stage in case of risk patients who are having genetic background of Glaucoma.

A. Sources of Image Dataset used for Development of Proposed Glaucoma Detection System

For our Glaucoma detection system experiments, analysis and testing results, we have used the Glaucomatous fundus image dataset and normal image dataset from the following sources:

High Resolution Fundus (HRF) image dataset, available on the public domain:
https://www5.cs.fau.de/research/data/fundus-images/.

This dataset has been established by a collaborative research group to support research and comparative studies on retinal fundus images [10], [11], which is used by many researchers for their experiments and testing results. This dataset comprises of a set of 15 Glaucoma and 15 Normal images and Fundus images available at KLE Dr. Prabhakar Kore Hospital, Belagavi, India, which have been captured using a Canon CF1 High Resolution fundus camera with a 50° field of view. Each image was captured using 24 bits per color plane at dimensions of 2534x2301 pixels.

We are referring the above two datasets in our thesis as (i) HRF dataset and (ii) Hospital dataset, respectively.

III. GLAUCOMA DETECTION USING TEMPLATE

This chapter presents an efficient methodology developed for the automatic localization and segmentation of the optic cup and disc in retinal images followed by extraction of some structural features for Glaucoma detection. Localization of the optic disc in the retinal image and extraction of the features is done by correlating the fundus image with a newly developed template using Pearson-r correlation. Segmentation of optic cup and disc is done on the basis of correlation levels [19], [21], [22], [23].

A. Pre-Processing

Our proposed methodology is based on correlating the fundus image with a designed template. The template is designed based on intensity distribution of fundus image. Hence, it is required to determine the intensity component of the input image. The RGB color format of the fundus image captured by the fundus camera does not reveal the intensity component value directly. Whereas, HSI (Hue, Saturation, Intensity) format representation of an image directly provide the intensity component value of an image (refer Figure 8). Therefore, the RGB format captured fundus image is converted into HSI format in the preprocessing stage. Conversion from RGB to HSI is achieved using following equations.

$$\mathrm{I(intensity)} = \frac{\mathrm{R(Red)+\ G(Green)+B(Blue)}}{3} \quad (1)$$

$$\mathrm{H(Hue)} = \cos^{-1}\left\{\frac{\frac{1}{2}[(\mathrm{R-G})+(\mathrm{R-B}]}{[(\mathrm{R-G})^2+(\mathrm{R-B})(\mathrm{G-B})]^{\frac{1}{2}}}\right\} \quad (2)$$

$$\mathrm{S(Saturation)} = 1 - \frac{3}{(\mathrm{R+G+B})}[\min(\mathrm{R,G,B})] \quad (3)$$

A sample RGB fundus image and its corresponding converted HSI image is shown in Figure 8.

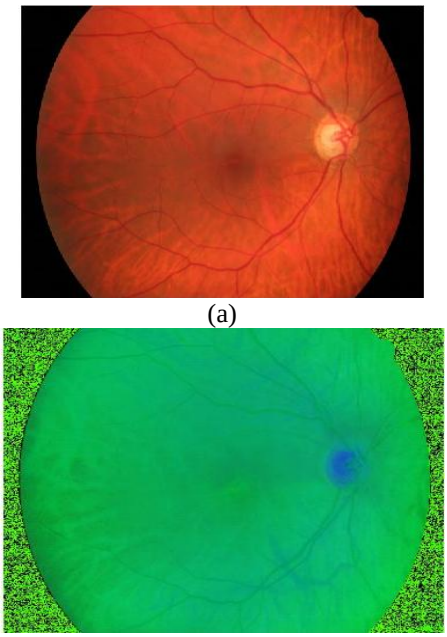

(a)

(b)

Fig. 8. Preprocessing stage (a) input fundus RGB image (b) converted HSI image

B. Glaucoma Detection using Pearson-r Coefficient Extraction

Further, the intensity component of the fundus image is correlated with a template designed using Pearson-r correlation to localize the optic disc in the image. The template is designed keeping in view the general structure of the optic disc and cup. The size of the optic disc varies significantly with the different fundus images. We observed that the optic disc widths varied from 60 to 100 pixels in the images of our dataset. The optic disc consists of a rim and cup. The intensity of the rim is higher compared to the rest of the image outside the rim and cup is the brightest part of the fundus image. We have designed a square shaped image template to have a disc with a rim and cup as shown in Figure 9(a). Cup will have the highest intensity and intensity decreases towards the rim and other outer parts of the image similar to intensity distribution pattern of a fundus image. A Laplacian of Gaussian distribution is used to get this intensity distribution pattern. Pearson-r coefficients are extracted from correlating the template with the preprocessed image. Correlated image contains the information of optic cup and disc in the form of intensity variation with respect to template image from the fundus image. As seen from Figure 8(b) for a sample correlated sample image, the optic disc and cup can be very easily separated on intensity plane.

The Laplacian of Gaussian distribution was generated such that intensity peaks at the center corresponding to the optic cup, as given by the equation,

$$\mathrm{T(x,y)} = \left(\frac{1}{\sigma^2}\right)[\left(\frac{x^2+y^2}{\sigma^2}\right) - 1)]\exp(-((x^2 + y^2)/2\sigma^2)) \quad (4)$$

Where, x is the distance from the origin in the horizontal axis, y is the distance from the origin in the vertical axis, and σ is the standard deviation of the Gaussian distribution. After getting the Gaussian distribution template, it is further scaled to generate the optic rim and cup with fixed widths by using the knowledge of the general widths of eye structure.

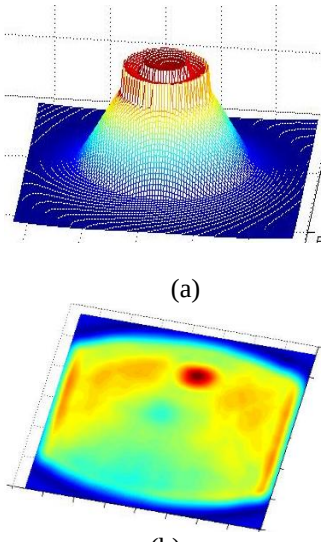

(a)

(b)

Fig. 9. Correlation (a) Correlation filter (b) Intensity distribution of correlated fundus.

Further, the optic cup and disc are easily segmented as they differ in their correlated magnitudes. Binary images of segmented optic disc, cup and rim are shown in Figure 10.

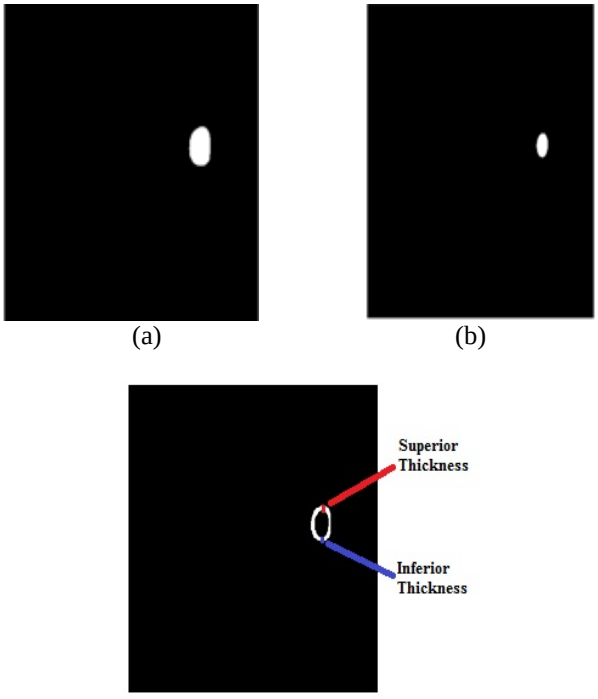

Fig. 10. Segmentation (a) Segmented Optic Disc. (b) Segmented Optic cup (c) Neuroretinal rim thickness.

Figure 11 and Figure 12 show the segmentation of optic cup and disc and Neuroretinal rim in binary image for a sample image of Hospital dataset and HRF dataset, respectively.

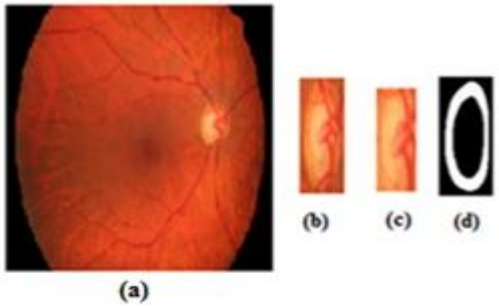

Fig. 11 (a) Original sample (b) Segmented Optic disc (c) optic cup (d) Binary image showing Neuroretinal rim.

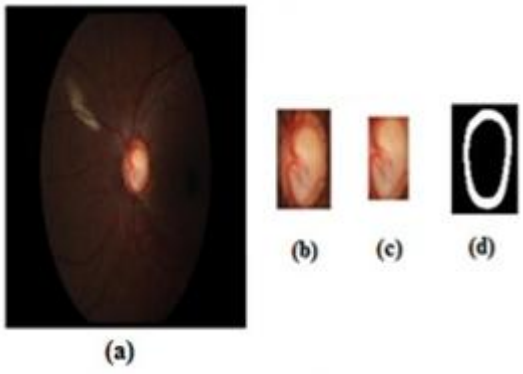

Fig. 12. (a) Original sample (b) Segmented Optic disc (c) Segmented optic cup (d) Binary image of Neuroretinal rim.

The values of CDR, RDR, and Superior and Inferior Rim thicknesses are calculated from the extracted image.

IV. GLAUCOMA DETECTION USING VESSEL SEGMENTATION

According to the literature survey due to progression of Glaucoma, blood vessels diameter decreases [13], [14], [24], [25] and smaller diameter vessels around the optic disc start diminishing and disappearing. Figure 13 clearly shows these aspects. The region where these significant vessels of interest are present in a small area around the optic disc in the image for detection of Glaucoma is considered as Region of Interest (ROI).

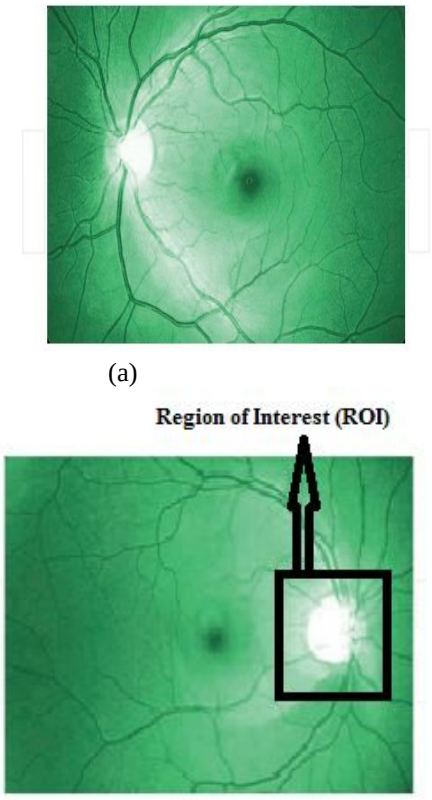

Fig. 13. Vessels in fundus image showing ROI (a) vessels in normal eye with smaller vessels around optic disc (b) absence of smaller vessels around optic disc in Glaucoma eye

We have employed these aspects of vessels as features to detect the Glaucoma at an early stage.

A. ROI Extraction

In previous section, we presented the methodology of segmenting the optic disc by correlating the input fundus image with designed template using Pearson-r correlation. The value of Pearson-r correlation is maximum at the center of the optic disc which corresponds to brightest spot in the fundus image. After segmenting the disc as discussed in Section B of template approach, its boundary points on the top, bottom, left and right sides are identified, thus localizing it. A sample fundus image from our dataset and corresponding identified ROI image part is shown in Figure 14.

(a) (b)

Fig. 14. (a). Input image (b) Extracted ROI.

In signal processing applications analysis of signal in frequency domain is preferred over the time domain since they contain more information of the signal. This requires conversion of the signal from time domain to frequency domain. Fourier transform can be used to obtain the frequency contents of a signal. But it does not reveal which frequency component is present at what time instance of the signal. Wavelet transform, on the other hand, reveals this information and convey more detailed information regarding the signal or the image. In image processing techniques such as segmentation, image decomposition using un-decimated bi-orthogonal wavelet transforms are employed, as these transforms also facilitate reconstruction of the images [26]. For segmentation of astronomical and biological images where images contain isotropic objects, the Isotropic Un-decimated Wavelet Transform (IUWT) can be applied for segmentation. In the fundus images, vessels are isotropic in nature. Hence IUWT can be used for segmentation of vessels. When ROI is subjected to IUWT, decompositions at different wavelet levels are as sown in Figure 15.

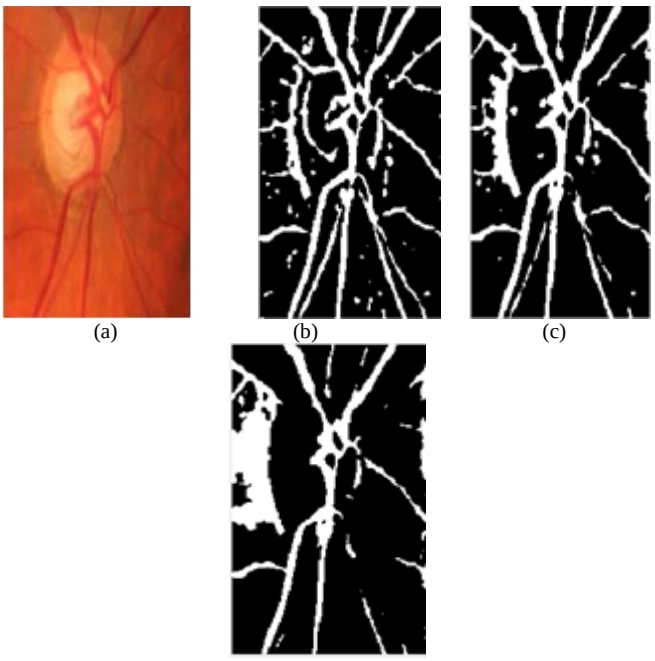

(a) (b) (c)

(d)

Fig. 15. (a) Extracted ROI. (b) Image with low wavelet level of 3 (c) Image with high wavelet level of 4 (d) Image with wavelet level of 5.

B. Vessel Localization

For further processing image with a wavelet levels of 3 is considered. To obtain the center line of each of the segmented vessels, they are subjected to a thinning process which converts a vessel into a thin vessel of one pixel thickness. The position of this thin vessel will be almost in the center of the vessel and it represents the center line of the vessel. A sample of segmented vessels of ROI is shown in Figure 16(a). The output of the thinning process of the sample vessels is shown in Figure 16(b), which depicts the thinned centerlines of vessels. Figure 16(c) depicts the identified thinned branches after removing the branch pixels. Each thin line in the image of Figure 16(c) represents a separate vessel. Now, each thin line in the image represents a separate vessel.

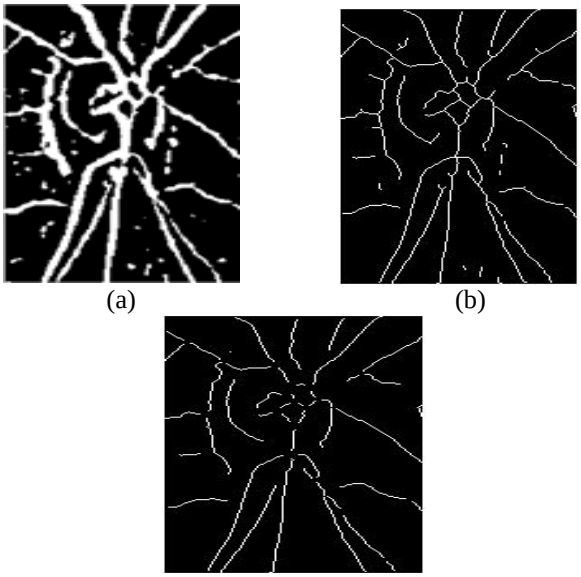

(a) (b)

(c)

Fig. 16. (a) Vessels from the segmented image (b) Thinned centerlines and (c) centerlines with branches separated.

Using connected components technique, each line (vessel) in the image is indexed and can be accessed with that index. Further, using the index information the coordinates of the centerline pixels of each vessel are determined, thereby localizing the vessels. Further, the vessel data structure is created and maintained which contains entire information regarding the vessels. Vessel based Feature VRI (Vessel Risk Index) is extracted from the information obtained in vessel data structure [23].

V. GLCM APPROACH FOR GLAUCOMA DETECTION

This section presents GLCM Approach for Glaucoma Detection. Here GLCM based texture features are extracted and fed to Neural Classifier. Neural Classifier is then trained to Classify input fundus image as either Normal or Glaucoma affected image.

A. Image Pre-processing

The fundus image captured from the camera is first converted into gray image. In order to eliminate impulse noise in the fundus image an adaptive weiner [] filter is used which often produces better results than linear filtering. It is also more effective in preserving the edges. It is a Pixel wise linear filter formed by estimating the local mean and variance around each pixel. The value of the restored image P at any point (i, j) is,

$$P(i,j) = \mu + \frac{(\sigma^2 - v^2)}{\sigma^2}(T(i,j) - \mu) \qquad (5)$$

Where μ is the mean of the area under consideration, σ2 is the variance, v2 is the noise variance and T is the image under consideration for removal of noise.

B. Feature Extraction using GLCM

A gray level co-occurrence matrix (GLCM) or co-occurrence distribution (less often co-occurrence matrix or co-occurrence distribution) is a matrix or distribution that is defined over an image to be the distribution of co-occurring values at a given offset. A GLCM is a matrix where the number of rows and columns is equal to the number of gray levels, G, in the image. The use of statistical features is therefore one of the early methods proposed in the image processing literature. Haralick [14] suggested the use of co-occurrence matrix or gray level co-occurrence matrix. It considers the relationship between two neighboring pixels, the first pixel is known as a reference and the second is known as a neighbor pixel. It is also called as grey tone spatial dependency matrix. It is used to determine the texture of an image, and it tabulates the brightness values of an image as how often they occur. Here we extract the 5 features mainly homogeneity, correlation, co-occurrence, energy and entropy. In GLCM there are mainly two pixel values are present and it considers the relation between them, those are reference pixel and neighbor pixel. The neighbor pixel is selected to be the one to the right of each reference pixel. The GLCM matrix is a square matrix with dimension Ni, where Ni=number of gray levels. element[j,k] is generated by calculating how many times the pixel value of j is adjacent to the pixel value of k, then it is divided by the total number of such comparisons made.

B.1 Contrast

It quantifies the local variations in the GLCM matrix. It defines the intensity contrast between a pixel and its neighbor in an entire image. The value of contrast is 'zero' for a steady image. This property of contrast is also known as inertia and variance. The contrast of an image is given by:

$$\text{Contrast} = \sum_{j,k} |j-k|^2 P(j,k)^2 \qquad (5)$$

Where j, k = reference pixel and neighbor pixel values, P=normalized value.

B.2 Correlation

It defines that how the pixel is correlated to its neighbor in an image. And also calculates the joint probability of the particular pixel pairs. The value of correlation ranges from -1 to +1.the positively correlated image has +1 value and negatively correlated image has -1 value, for constant images correlation has no value.

$$\text{Correlation} = \frac{\sum_{j,k}(j-\mu j)\,(k-\mu k)\,P(j,k)}{\sigma j \sigma k} \qquad (6)$$

Where μ =mean in the GLCM image and σ the variance

B.3 Energy

It gives the value of sum of square elements in the GLCM.the range of energy is between 0 and 1.the energy is also called as uniformity or the angular second moment. The energy in GLCM is given by

$$\text{Energy} = \sum_{j,k} P(j,k)\text{^}2 \qquad (7)$$

B.4 Homogeneity and Angular Secondary Moment

This feature gives extent of homogeneity in an image. It measures the distance of the allotment of elements in the GLCM to the GLCM diagonal. The value of homogeneity ranges from 0 to 1 and is 1 for diagonal GLCM values. It is given by,

$$\text{ASM} = \sum_{i=0}^{G-1} \sum_{j=0}^{G-1} P(i,j)\text{^}2 \qquad (8)$$

Where, G represents Gray levels in an image.

B.5 Entropy

The entropy is calculated from logarithm of base 2.here we can use less number of bits to predetermine the local grey level distribution. The entropy is given by

$$\text{Entropy} = \sum_{j,k} P(j,k) \log (P(j,k)) \qquad (9)$$

C. Neural Classifier

Classification using ANN is the state-of-the-art technique employed for efficient classifications. We have used feed forward ANN with modified back propagation training technique to implement the classifier. Feed forward Multiple Layer Perceptron (MLP) neural networks are one of the important types of neural networks. They are widely used in recognition systems due to their good generalization property. MLPs consist of multiple layers as shown in Figure 19. It has one input and one output layer. One or more hidden layers are used in between input and output layers. The number of neurons in the input layer depends on the number of inputs to be fed to the network and the number of neurons in the output layer depends on the number of outputs to be generated for the final classifier output. Hidden layers can have any number of neurons. Output of a neuron of input/hidden layer is connected to the input of all neurons in the next layer in fully connected network, as shown in Figure 18.

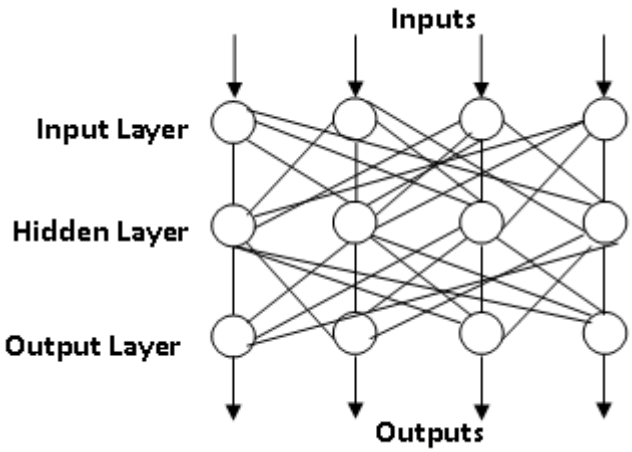

Figure 18. Feed forward neural network

D. Glaucoma Neural Classifier Architecture

We used a 2-layer MLP with two hidden layer and one output layer. For each input fundus image 5 GLCM features are extracted and fed to Input Layer. As the output result we want it to be either Normal or Glaucoma indication, the output layer consists of only one neuron. We used two hidden layers with 5 neurons in each layer as we could get better results with two hidden layers than one. The architecture of the neural classifier used is shown in Figure 19.

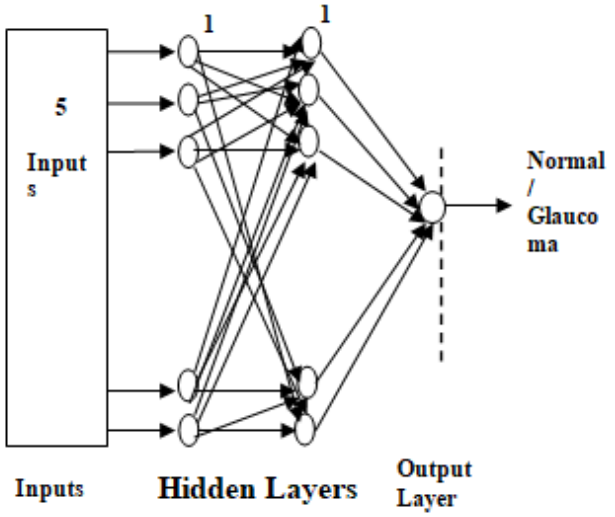

Figure 19. Architecture of Glaucoma neural classifier

Different training methods can be used to train the MLPs for classification. We employed the modified popular back propagation training algorithm with the minimum mean square error performance as a function for training our neural classifier. Levenberg-Marquardt method [16], [17] of optimization is used to train the classifier.

VI. RESULTS & DISCUSSION

Our final proposed integrated Glaucoma classifier system considers all these proposed features for classification. The structural features related to optic disc and cup such as CDR, RDR, Superior and Inferior rim thicknesses, which are extracted using template methodology. VRI, the vessel structural feature and Texture features obtained by GLCM technique. This aspect of incorporating more features has led to improvement of the efficiency of Glaucoma detection which can be seen from comparison of results as shown in the Table 1. Totally, 120 Glaucoma images and 60 Normal images were used from the datasets consisting of both private and public dataset for comparison.

Table 1. Results of Glaucoma classifier

Image Type inclusive of Proprietary and Public Data sets	Results of feature extraction using NSK Template	Results of using Vessel based feature VRI	Results of using GLCM and Neural classifier	Results of Final Integrated Glaucoma classifier
Glaucoma dataset	94%	85%	95%	98.57%
Normal dataset	90%	83%	94%	94%

We also compared our results of Final Integrated Glaucoma classifier with Glaucoma Detection using Wavelets and SVM Classifier [18] on the same dataset. Results of the approach reported in [18] were 95% on Glaucoma Dataset and 90% on Normal dataset respectively.

VII. CONCLUSIONS

Literature survey reveals that previously attempts were made to detect Glaucoma by extracting predominantly CDR or wavelet based features. We have also improved the efficiency of CDR based Glaucoma detection system by a template for correlation with input fundus images. As seen from results section, template correlation approach is better when compared to intensity threshold techniques. Additional features; RDR and neuroretinal rim thickness have improved the efficiency of the system.

We have introduced vessel based features for Glaucoma detection which is a significant step towards Glaucoma detection. As seen in the literature, reductions in vessel diameters are the indication of Glaucoma. To detect this we have incorporated database where these significant features can be stored and monitored for regular visits of patients. GLCM based strategy has also been used by us to increase the efficiency of the system. We have used artificial neural networks to classify the input fundus images using wavelet based textures.

In our research work of Glaucoma detection, we have enhanced the efficiency of Glaucoma detection system by processing and analyzing additional fundus image features apart from the CDR or GLCM features leading to a hybrid approach.

ACKNOWLEDGMENTS

We would like to express our sincere gratitude to Dr. Rekha Mudhol, Ophthalmology department of K. L. E. Society's Dr. Prabhakar Kore Hospital & M.R.C., Belagavi, India for providing us with necessary guidance and resources required for experimentation. We would like to thank Dr Dileep Kumar, Manager, MR Research & Collaborations, Seimens Healthineers, Bangalore for the guidance provided. Special thanks to High Resolution Fundus (HRF) Image Database available on internet [10].

REFERENCES

1. Raychaudhuri A, Lahiri SK, Bandyopadhyay M, Foster PJ, Reeves BC, Johnson GJ. A Population Based Survey of the Prevalence and Types of Glaucoma in Rural West Bengal. The West Bengal Glaucoma Study. The British Journal of Ophthalmology. 2005; 89:12. 1559–1564.
2. Xiaoyang Song,Keou Song, Yazhu Chen. A Computer-based Diagnosis System for Early Glaucoma Screening. Proc. IEEE Engineering in Medicine and Biology 27th Annual Conf. 2005; pp. 6608-6611.
3. Eye Anatomy. Available from http://www.optos.com/en-US/Patients/Healthy-sight /Eye-anatomy/ [Accessed: 2016-12-15]
4. Guyton, A. C. and J. E. Hall. Textbook of Medical Physiology. Elseveir Saunders. 9th edition. 1996.
5. Malaya Kumar Nath, Samarendra Dandapat. Techniques of Glaucoma Detection from Color Fundus Images: A Review. International Journal of Image, Graphics and Signal Processing. Vol. 4, 2012; 44-51. DOI: 10.5815.
6. M. Mishra, M. K. Nath, S. R. Nirmala, S. Dandapat. Image Processing Techniques for Glaucoma Detection. Communications in Computer and Information Science:

Advances in Computing and Communications: Springer. Vol. 192. 2011; 365-373.
7. Jost D. Jonas, Xuan N.Nguyen, Gottfried O. H. Naumann. Parapapillary Retinal Vessel Diameter in Normal and Glaucoma Eyes: Morphometric data. Investigative Ophthalmology & Visual Science, Vol.30, No.7, 1989; 1599-1603.
8. Jennifer K. Hall, md, Anthony P. Andrews, md, Rebecca Walker, md, Jody r, Piltz-seymour, md. Association of Retinal Vessel Caliber and Visual Field Defects in Glaucoma. Am J Ophthalmol, Vol.132, No.6, 2001; 857-859.
9. S. Dua, U. R. Acharya, E. Y. K. Ng, Computational Analysis of the Human Eye With Applications. World Scientific Press. 2011.
10. Attila Budai, Jan Odstrcilik, High-Resolution Fundus (HRF) Image Database. https://www5.cs.fau.de/ research/data/fundus-images/.
11. Jan Odstrcilik, Radim Kolar, Attila Budai, Joachim Hornegger, Jiri Jan, Jiri Gazarek, Tomas Kubena, Pavel Cernosek, Ondrej Svoboda, Elli Angelopoulou. Retinal vessel segmentation by improved matched filtering: evaluation on a new high-resolution fundus image database. IET Image Processing, Volume 7, Issue 4, June 2013; 373-383, DOI: 10.1049/iet-ipr.2012.0455.
12. J. Nayak, Rajendra Acharya U, P. S. Bhat, N. Shetty, T.-C. Lim. Automated Diagnosis of Glaucoma Using Digital Fundus Images. Journal of Medical Systems. Springer. Vol. 33. 2009; 337-346. DOI: 10.1007/s10916-008-9195-z2009.
13. L´aszl´oG.Ny´ul. Retinal image analysis for automated Glaucoma risk evaluation. Medical Imaging, Parallel Processing of Images, and Optimization Techniques, edited by Jianguo Liu, KunioDoi, Aaron Fenster, S. C. Chan. Proc. of SPIE. Vol. 7497, 2009; 74971C-1 to 74971C-9. DOI: 10.1117/12.851179.
14. Y. Xu, D. Xu, S. Lin, J. Liu, J. Cheng, C. Y. Cheung, T. Aung, T. Y. Wong. Sliding Window and Regression Based Cup Detection in Digital Fundus Images for Glaucoma Diagnosis. Springer-Verlag. Part III. LNCS 6893. 2011; pp. 1-8.
15. S. Dua, U. R. Acharya, P. Chowriappa, S. V. Sree. Wavelet-Based Energy Features for Glaucomatous Image Classification. IEEE Transactions on Information Technology in Biomedicine. Vol. 16. 2012; 80-87. DOI: 10.1109/TITB.2011.2176540.
16. Levenberg, Kenneth. "A method for the solution of Certain Non-Linear Problems in Least Squares. Quarterly of Applied mathematics. Volume 2. 1944; 164-168.
17. Auer, Peter, Harald Burgsteiner, Wolfgang Maass. A learning rule for very simple universal approximators consisting of a single layer of perceptrons. Neural Networks. 21 (5). 2008; 786–795.
18. Nataraj Vijapur, Smita Chitins, R. Srinivasa Rao Kunte. Improved Efficiency of Glaucoma Detection by using Wavelet Filters, Prediction and Segmentation Method. International Journal of Electronics, Electrical and Computational System. Academic Science Publishers. Volume 3. Issue 8. Oct 2014; 1-13.
19. Lowell J, Hunter A, Steel, D. Basu, A, Ryder R, Fletcher, E. Kennedy, L. Optic nerve head segmentation. IEEE Transactions on Medical Imaging, vol. 23. no. 2. Feb 2004; 256-264.
20. Uhm KB, Lee DY, Kim JT, Hong C. Peripapillary atrophy in normal and primary open-angle glaucoma. Korean J Ophthalmol. Jun 1998; 37-50.
21. Real Statistics Using Excel: Correlation: Basic Concepts, Available: http://www.real-statistics.com/correlation/. [Accessed: 2015-02-22]
22. Nataraj A Vijapur, R. Srinivasa Rao Kunte. Glaucoma Detection by Using Pearson-R Correlation Filter. Proc. 4th IEEE International Conference on Communication and Signal Processing (ICCSP'15). April 2015; 1194-1198. DOI: 10.1109/ICCSP.2015.7322695.
23. Vijapur, N.A. & Kunte, R.S.R. Sensitized Glaucoma Detection Using a Unique Template Based Correlation Filter and Undecimated Isotropic Wavelet Transform,. J. Med. Biol. Eng. (2017) 37: 365. https://doi.org/10.1007/s40846-017-0234-4
24. Patton N, Aslam TM, MacGillivray T, Deary IJ, Dhillon B, Eikelboom RH, Yogesan K, Constable I J. Retinal image analysis: concepts, applications and potential. ProgRetin Eye Res., Epub. 2005; 99-127.
25. Seoung-Block Lee, Ki Bang Uhmandand Chul Hong. Retinal Vessel Diameter In Normal and Primary Open Angle Glaucoma. Korean J. Opthalmol. Vol. 12. 1998; 51-59.
26. Jean-Luc Starck, Jalal Fadili, FionnMurtagh. The Undecimated Wavelet Decomposition and its Reconstruction. IEEE Transactions On Image Processing. Vol. 16. No. 2. Feb. 2007; 297-309.

AUTHORS PROFILE

Dr. Nataraj Vijapur pursued B.E in Electronics & Communication, M.Tech in VLSI Design and Embedded Systems and Doctorate in Image Processing and Classification systems on Fundus image Processing. His research interests include Image Processing Systems, Machine learning Models for VLSI systems and VLSI Architectures for machine learning systems. He is Life time member of Association of ISTE. He has 18 years of Teaching experience and serving KLE Dr M.S.Sheshgiri College of Engineering and Technology, Karnataka, India. He has handled University Member of Board of Examination in UG & PG schemes. He has published several peer reviewed international journal and conference papers. He is reviewer of many Journals and Organized many Conferences, Seminars and Workshops.

Dr. Srinivasa Rao Kunte pursued B.E in Electronics & Communication, M.Tech in Industrial Electronics and Doctorate in Online handwritten Kannada Characters/Script Recognition. His research interests include Character/Pattern Recognition, Efficient Glaucoma detection system and Vector Quantization for efficient Real time Image compression systems. He is Life time member of Associations FIETE., MIEEE. And MISTE. He has developed a unique, efficient, useful and first of its kind system 'On-Line Handwritten Character Recognition System' for Kannada and other Indian languages to recognize the handwritten characters written on a Digitizer pad. He has 36 years of Teaching experience with 11 years as Head of the institution and responsible for development, growth and recognition of JNN college of Engineering, Shivamogga, Karnataka, India. He has handled University Assignments as Academic Senate member, Chairman and Member of Board of Studies in formation of Electronics and Telecommunication syllabus for many UP & PG schemes. He is a Chairman of Affiliation Inspection committee; Active member of IETE professional body and responsible for starting IETE Students' Forum, PAC centre, Sub-centre and Centre at Shivamogga; He has published several peer reviewed international journal and conference papers. He is reviewer of many Journals and Organized many Conferences, Seminars and Workshops.